

Original articles

Research article

<https://doi.org/10.17308/kcmf.2023.25/11473>

Pair interaction of intersecting dilatation and disclination defects

S. A. Krasnitskii^{✉1}, A. M. Smirnov¹

¹ITMO University,
49 Kronverksky pr., bldg. A, St. Petersburg 197101, Russian Federation

Abstract

An elastic interaction of the intersecting dilatation and disclination defects located in an infinite linear isotropic media is investigated. The eigenstrain approach is employed to obtain the analytical expressions describing the pair interaction between intersecting dilatational lines and intersecting wedge disclinations. It is demonstrated that the interaction energy strongly depends on the intersection angle between the defects. The energy reaches the maximum value if the defect lines are coincided while the energy reaches the minimum value if the defect lines are orthogonal. Besides, it is shown that interaction energy of intersecting wedge disclinations strongly depends on the elastic properties of the media: the less the Poisson ratio, the less the energy. The obtained analytical results seem to be applicable for the theoretical analysis of the residual stress relaxation mechanisms in heterostructures with pentagonal symmetry such as icosahedral particles.

Keywords: Disclination, Dilatation line, Pair interaction

Funding: The study was supported by the Russian Science Foundation, project No 23-72-10014.

For citation: Krasnitskii S. A., Smirnov A. M. Pair interaction of intersecting dilatation and disclination defects. *Condensed Matter and Interphases*. 2023;25(4): 505–513. <https://doi.org/10.17308/kcmf.2023.25/11473>

Для цитирования: Красницкий С. А., Смирнов А. М. Энергия парного взаимодействия пересекающихся дефектов дилатационного и дисклинационного типа. *Конденсированные среды и межфазные границы*. 2023;25(4): 505–513. <https://doi.org/10.17308/kcmf.2023.25/11473>

✉ Stanislav A. Krasnitskii, e-mail: krasnitsky@inbox.ru

© Krasnitskii S. A., Smirnov A. M., 2023



The content is available under Creative Commons Attribution 4.0 License.

1. Introduction

Due to the unique functional properties, inhomogeneous nanostructures are widely used in the design of modern electronic devices [1], photonics [2] and plasmonics [3]. The stability of the properties of such nanostructures is mainly determined by crystal defects that arise during the relaxation of mechanical stresses [4–7]. The main mechanisms of stress relaxation include the formation of point defects complexes [8, 9], generation of dislocation [10–17] and disclination [18–20] configurations, nucleation of cracks and various V-shaped defects [21–23], diffusion perturbation of the surface [21, 24].

The processes of stress relaxation in inhomogeneous particles with fifth-order symmetry axes (pentagonal prism, decahedron and icosahedron) are of particular interest [25, 26]. The residual strains and stresses attributed to these particles are caused by five-fold twinning around the fifth-order symmetry axes and can be described within the framework of the disclination concept [27, 28]. According to this concept, pentagonal whiskers and decahedral particles contain one positive wedge disclination with strength 0.128 rad, (the disclination axis coincides with the symmetry axis of the fifth order), while icosahedral particles contain six positive wedge disclinations with strength 0.128 rad, passing through the opposite apexes of the icosahedron and intersecting at its centre. The elastic field of wedge disclination as a strong sink have a significant influence on point defect migration. Therefore, on the initial stages of residual stress relaxation, the formation of atmospheres of impurity atoms and vacancies along the cores of wedge disclinations can be expected. On the following stages of relaxation process the concentration of vacancies (impurity atoms) can reach essential enough supersaturation to condense to pores (second phase nuclei), that was observed experimentally [29, 30] and theoretically described in [32–34].

Thus, an analysis of the initial stages of residual stress relaxation due to the segregation of point defects on the disclination cores in icosahedral particles can be performed through the determination of the interaction energies of the defects under consideration. This study presents

analytical expressions for the pair interaction energies of the following defect configurations: intersecting dilatation lines and intersecting wedge disclinations placed in the infinite medium. Despite the fact that the obtained results are valid for the infinite medium assumption, they can be used as a starting point for calculating the energy of the pair interactions of intersecting defects in finite bodies with a free surface in future.

2. Theoretical part

In this section an elastic isotropic medium containing intersecting direct defects, such as dilatation lines and wedge disclinations is considered. The energy of the pair interactions of these defects can be defined as the work spending on the generation of one of the defects in the stress field of another defect [35]:

$$W_{\text{int}}^{I-II} = -\int_V \beta_{ij}^I \sigma_{ij}^{II} dV = -\int_V \beta_{ij}^{II} \sigma_{ij}^I dV, \quad (1)$$

where β_{ij}^I and β_{ij}^{II} are components of the plastic distortion tensor of the defects (I) and (II), σ_{ij}^I and σ_{ij}^{II} are components of the elastic stress tensor of the defects (I) and (II), induced in the material volume V .

2.1. Energy of the pair interactions of intersecting dilatation lines

Consider the straight dilatation lines L_I and L_{II} , intersecting at a point O under the angle α (Fig. 1a). We introduce the Cartesian coordinate systems $Oxyz$ and $Oxy'z'$, associated with lines of defects L_I and L_{II} respectively (axis x is perpendicular to the intersection plane of defects, axes z and z' coinciding with the lines of defects L_I and L_{II} , direction of axes y and y' prescribed by the right-hand rule). The stress field of these defects in an infinite elastic medium is known (see, for example, [36]). The non-zero components of the stress tensor of the dilatation line L_I in the Cartesian coordinate system can be presented in the following way:

$$\sigma_{xx}^{L_I} = -C_0 \xi^2 \frac{x^2 - y^2}{(x^2 + y^2)^2}, \quad (2a)$$

$$\sigma_{yy}^{L_I} = -C_0 \xi^2 \frac{y^2 - x^2}{(x^2 + y^2)^2}, \quad (2b)$$

$$\sigma_{zz}^{L_I} = -2C_0 H(\xi - x)H(\xi - y), \quad (2c)$$

$$\sigma_{xy}^{L_I} = -C_0 \xi^2 \frac{2xy}{(x^2 + y^2)^2}, \quad (2d)$$

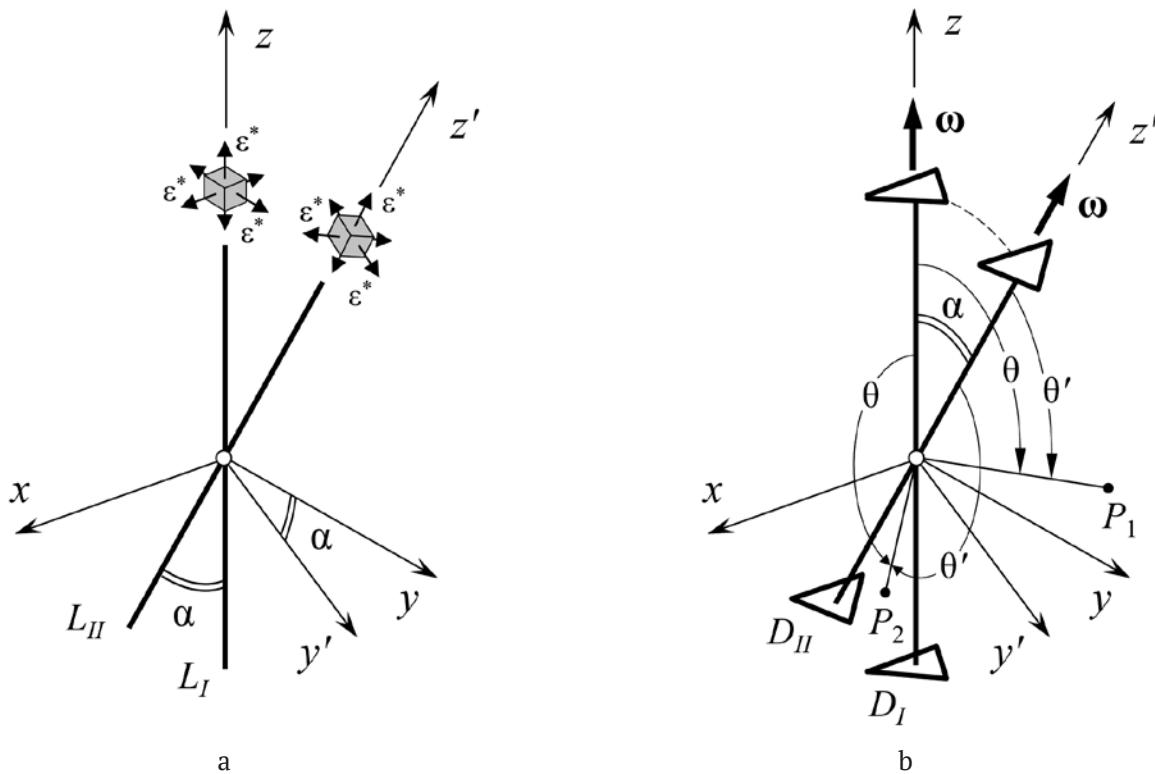


Fig. 1. An elastic model of the defects with an intersection angle α : a) dilatation lines L_I and L_{II} subjected to 3D eigenstrain ϵ^* ; b) wedge disclinations D_I and D_{II} with strength ω . Points P_1 and P_2 belong to areas $S_1 = \{R \geq 0, \varphi = \pi/2, \alpha \leq \theta \leq \pi\}$ and $S_2 = \{R \geq 0, \varphi = 3\pi/2, \pi - \alpha \leq \theta' \leq \pi\}$ respectively

where $C_0 = G\epsilon^*(1+\nu)/(1-\nu)$, G is a shear modulus; ν is a Poisson ratio; ϵ^* is a dilatation eigenstrain of the defect; $H(\dots)$ is a Heaviside function; ξ is a small parameter defining the radius of the core of the dilatation defect line. Expression (2c) for the axial component of the dilatation line stress tensor is a generalized function: the stress equals zero at all points of the medium, except for the points corresponding to the line of the dilatation defect.

The eigenstrain distortion of the dilatation line is characterized by triaxial deformation ϵ^* , distributed along the lines of defects. According to [36], non-zero components of the eigenstrain distortion of the dilatation line (II) can be expressed as:

$$\beta_{ii}^{L_{II}} = \epsilon^* s \delta(x) \delta(y'), \tag{3}$$

where $s = \pi \xi^2$, $\delta(\dots)$ is a one-dimensional Dirac delta function.

To determine the pair interaction specific energy of intersecting dilatation lines L_I and L_{II} we substitute (2) and (3) in the expression (1) for energy:

$$\begin{aligned} \tilde{W}_{\text{int}}^{L_I-L_{II}} &= -\int \beta_{ij}^{L_{II}} \sigma_{ij}^{L_I} dS = \\ &= 4\epsilon^* s C_0 \int \int H(\xi-x) H(\xi-y) \delta(x) \delta(y') dx dy = \tag{4} \\ &= 4\epsilon^* s C_0 \int_{-\xi}^{\xi} \delta(x) dx \int_{-\xi}^{\xi} \delta(y') dy. \end{aligned}$$

The first integral in (4) is taken by the definition of the Dirac delta function, the second is taken by using a change in variable $y = y' \cos \alpha$. Finally, we obtain:

$$\tilde{W}_{\text{int}}^{L_I-L_{II}} = 4\epsilon^* s C_0 |\cos \alpha|. \tag{5}$$

Let us consider the specific case when the defect lines L_I and L_{II} are orthogonal ($\alpha = \pi/2$). In this case, the total interaction energy of defects can be determined using the expression (1), with $y' = z$ we have:

$$\begin{aligned} W_{\text{int}}^{L_I-L_{II}}|_{\alpha=\pi/2} &= \\ &= 4\epsilon^* s C_0 \int \int \int H(\xi-x) H(\xi-y) \delta(x) \delta(z) dx dy dz = \tag{6} \\ &= 4\epsilon^* s C_0 \int_{-\xi}^{\xi} \delta(x) dx \int_{-\xi}^{\xi} dy \int_{-\infty}^{+\infty} \delta(z) dz. \end{aligned}$$

Finally, we obtain the energy of the pair interaction of dilatational lines intersecting under right angles:

$$W_{\text{int}}^{L-II} \Big|_{\alpha=\pi/2} = 8\varepsilon^* s\xi C_0. \tag{7}$$

2.2. Energy of the pair interactions of intersecting wedge disclinations

The wedge disclinations D_I and D_{II} with equal moduli of Frank vectors is considered. The disclination axes intersect at the point O under the angle α . The axes of Cartesian coordinate systems $Oxyz$ and $Oxy'z'$ are similar to the previous section (see Fig. 1b).

Elastic stress fields of wedge disclinations in an infinite medium are known (see, for example, [28] and [37]). The non-zero components of the wedge disclination stress tensor in a spherical coordinate system are given below:

$$\sigma_{xx}^{D_I} = C_1 \left(\frac{\nu}{1-2\nu} + \frac{y^2}{r^2} + \log r \right), \tag{8a}$$

$$\sigma_{yy}^{D_I} = C_1 \left(\frac{\nu}{1-2\nu} + \frac{x^2}{r^2} + \log r \right), \tag{8b}$$

$$\sigma_{zz}^{D_I} = C_1 \left(\frac{\nu}{1-2\nu} + 2\nu \log r \right), \tag{8c}$$

$$\sigma_{xy}^{D_I} = -C_1 \frac{xy}{r^2}, \tag{8d}$$

where $C_1 = G\omega/[2\pi(1-\nu)]$, ω is a disclination strength; polar radius $r = (x^2 + y^2)^{1/2}$. As can be seen from expressions (8), the stress field components of a wedge disclination located in an infinite elastic medium are characterized by logarithmic singularity. This singularity can be eliminated by incorporating self-screening systems, for instance, the disclination dipoles and quadrupoles [38] and the disclinations in finite bodies bounded by cylindrical [38] or spherical [39] surfaces.

The plastic distortion of the wedge disclination D_{II} is defined on the half-plane as $S_{II} = \{x = 0, y' > 0, z'\}$. The non-zero component of the disclination plastic distortion tensor D_{II} is:

$$\beta_{xx}^{D_{II}} = -\omega y' \delta(x) H(S_{II}), \tag{9}$$

where $H(S_{II})$ is the two-dimensional Heaviside function equal to 1 at $x, y \in S_{II}$ and equal to 0 at $x, y \notin S_{II}$.

Taking into account (8) and (9), the energy of the pair interaction of intersecting wedge disclinations D_I and D_{II} can be expressed:

$$\begin{aligned} W_{\text{int}}^{D_I-II} &= \omega \iiint_{-\infty}^{+\infty} \sigma_{xx}^{D_I} y' \delta(x) H(S_{II}) dx dy' dz' = \\ &= \omega \int_{-\infty}^{+\infty} \int_0^{+\infty} \sigma_{xx}^{D_I} \Big|_{S_{II}} y' dy' dz'. \end{aligned} \tag{10}$$

Spherical coordinates (R, φ, θ) and (R, φ', θ') with the origin at the point O are introduced. Polar (colatitude) angles θ and θ' are measured from the axes by disclination D_I and D_{II} accordingly ($0 \leq \theta, \theta' \leq \pi$). Azimuthal angles φ and φ' are measured from the axis x ($0 \leq \varphi, \varphi' \leq 2\pi$). Taking into account the relationship between spherical and Cartesian coordinates: $y' = R \sin \theta', z' = R \cos \theta', dy' dz' = -RdRd\theta'$, we present (10) in the following form:

$$W_{\text{int}}^{D_I-II} = -\omega \int_0^A \int_0^\pi \sigma_{xx}^{D_I} \Big|_{S_{II}} \sin \theta' d\theta' R^2 dR, \tag{11}$$

where A – parameter, in the case of an infinite medium $A \rightarrow +\infty$.

It is worth noting that in the coordinate system associated with the disclination D_I , the half-plane S_{II} is determined by the sum of regions $S_1 = \{R \geq 0, \varphi = \pi/2, \alpha \leq \theta \leq \pi\}$ and $S_2 = \{R \geq 0, \varphi = 3\pi/2, \pi - \alpha \leq \theta \leq \pi\}$. With respect to the change of variable $\theta' = 2\pi - \alpha - \theta, d\theta' = -d\theta$ at $\pi - \alpha \leq \theta \leq \pi$. And $\theta' = \theta - \alpha, d\theta' = d\theta$ at $\alpha \leq \theta \leq \pi$, we present integral (11) as a sum of integrals over regions S_1 and S_2 :

$$W_{\text{int}}^{D_I-II} = -\omega \int_0^A \left(\int_{\pi-\alpha}^\pi \sigma_{xx}^{D_I} \Big|_{S_1} \sin(\theta + \alpha) d\theta + \int_\alpha^\pi \sigma_{xx}^{D_I} \Big|_{S_2} \sin(\theta - \alpha) d\theta \right) R^2 dR. \tag{12}$$

Integrals in (12) with regard to (8a) and $x = 0, y = R \sin \theta$ can be calculated analytically, for example, using tables of integrals [40]. Here we present the final expression for the interaction energy stored by wedge disclinations D_I and D_{II} in a subregion bounded by the surface of a sphere of radius A :

$$W_{\text{int}}^{I-II} = \omega C_1 \frac{A^3}{3} \left[-\frac{1-5\nu}{3(1-2\nu)} - \cos \alpha \ln \left(\tan \frac{\alpha}{2} \right) + \log(A \sin \alpha) \right]. \tag{13}$$

To determine the energy density of the interaction of disclinations D_I and D_{II} stored in a sphere of radius A , we divide expression (13)

by the volume of the sphere and present it in the following form:

$$w_{int}^{D_I-II} = w_A + w_\alpha, \tag{14}$$

where the first term contains a logarithmic singularity of disclination-type defects determining the contribution of the scale factor to the disclination interaction energy:

$$w_A = \frac{\omega C_1}{4\pi} \log A, \tag{15}$$

the second term contains the dependence of the interaction energy density of the disclination D_I and D_{II} on the angle between them:

$$w_\alpha = \frac{\omega C_1}{4\pi} \left[-\frac{1-5\nu}{3(1-2\nu)} + \cos\alpha \log(1+\cos\alpha) + (1-\cos\alpha)\log(\sin\alpha) \right]. \tag{16}$$

Thus, analytical expressions (14), (15), and (16) were obtained for the interaction energy density of intersecting disclinations in an infinite medium. Equation (15) expresses the dependence of the interaction of energy density on the size of the considered region: the interaction energy density increases according to the logarithmic law if the size of the considered region increases ($w_A \sim \log A$ at $A \rightarrow +\infty$). For the case of finite bodies (particles, whiskers, etc.), the expression (15) is modified due to screening effect of the surfaces, and the energy density w_A has a finite value (see, for example, similar calculations for the disclination energy in an elastic sphere [41]). The equation (16) shows the influence of the angle between disclinations α on the energy of pair interactions and it is the main interest of this study.

3. Results and discussion

Let us proceed to the analysis of the obtained expressions (5) and (7) for the energies of the pair interaction of intersecting dilatation lines L_I and L_{II} . The specific interaction energy of defects depending on the angle between them is shown in Fig. 2. Energy of interaction $\tilde{W}_z^{L_I-II}$ takes the highest value for angles $\alpha = 0, \pi$ and equals to the linear elastic energy of one dilatational line with its eigenstrain deformation $2\varepsilon^*$. The specific energy takes the zero value when the lines of defects intersect under right angles ($\alpha = \pi/2$). In this specific case, the interaction of defects

is determined by the total energy of the system presented in (7). Thus, it can be inferred that the interaction of dilatation lines intersecting under right angles is completely determined by their total eigenstrain deformation at the point of their intersection; the remaining sections do not contribute to the total interaction energy. It is worth noting that the energy of the pair interaction in (7) is equal to doubled elastic energy of a point defect with its triaxial eigenstrain ε^* .

Now turn to the dependences of the interaction energy density of intersecting wedge disclinations. In Fig. 3a the dependences of the normalized energy density w_α on the value of the angle between them α , plotted for different values of the Poisson ratio of the medium $\nu = 0.1$ and 0.3 are shown. According to Fig. 3a it can be seen that the energy densities take the smallest value ($\sim 0.6G\omega^2/(4\pi^2)$ for $\nu = 0.3$) in the case when the disclination axes intersect under right angles. On the contrary, the energy densities take the greatest value ($\sim 1.6G\omega^2/(4\pi^2)$ for $\nu = 0.3$) in the case when the disclination axes coincide ($\alpha = 0, \pi$). Here we present analytical formulas for determining the interaction energy density of disclinations intersecting under angles $\alpha = \pi/2$ and $0, \pi$, obtained from expression (16):

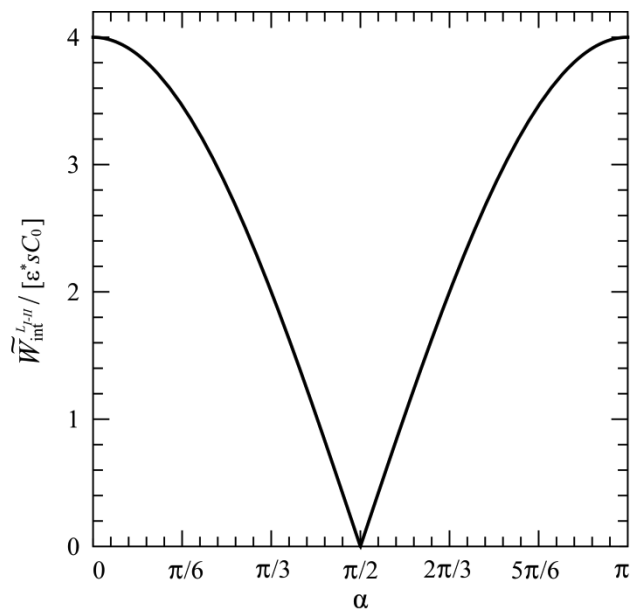


Fig. 2. Specific interaction energy of intersecting dilatational lines in dependence on the angle α . The energy is given in units $\varepsilon^* s C_0$

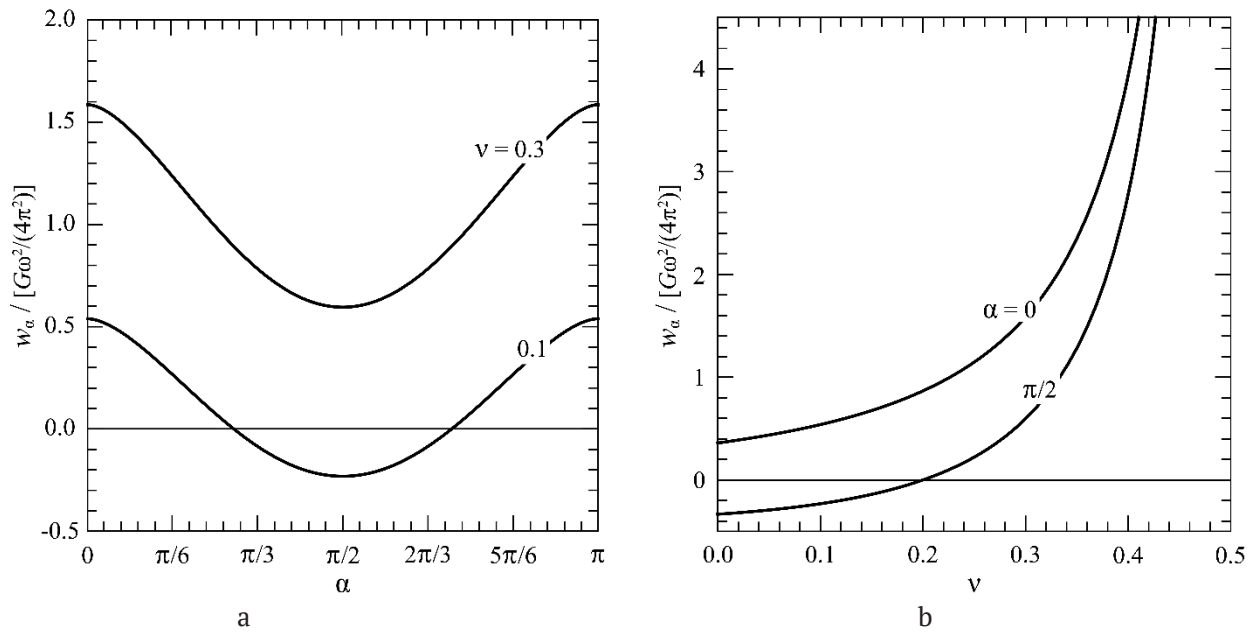


Fig. 3. Dependences of the interaction energy density of intersecting wedge disclinations w_α : a) on the intersection angle α for $\nu = 0.1$ and 0.3 ; b) on the Poisson ratio ν of the elastic medium for $\alpha = 0$ and $\pi/2$. The energy density is given in units $G\omega^2/(4\pi^2)$

$$w_{\alpha=\pi/2} = \frac{G\omega^2}{4\pi^2(1-\nu)} \left[-\frac{1-5\nu}{3(1-2\nu)} \right], \quad (17)$$

$$w_{\alpha=0,\pi} = \frac{G\omega^2}{4\pi^2(1-\nu)} \left[-\frac{1-5\nu}{3(1-2\nu)} + \log 2 \right]. \quad (18)$$

Expression (18) can also be used to determine the part of the elastic energy density of a disclination with strength of 2ω independent of R .

In addition, we note that according to Fig. 3a, disclinations located in elastic space with a relatively large Poisson ratio ν has a higher energy density: with increasing ν , the interaction energy density w_α increases. Let us turn to the dependences of the energy density of the interaction of disclinations w_α from the Poisson ratio of the medium ν ($0.0 < \nu < 0.5$), presented in Fig. 3b. In the case when the disclination axes coincide ($\alpha = 0$ or π), the interaction energy density is positive. On the contrary, in the case when the disclination axes intersect under right angles ($\alpha = \pi/2$), the interaction energy density can take negative values. The value of Poisson ratio, at which the energy density changes sign, is determined from expression (17) and equal to 0.2 . This means that in media with a relatively low Poisson ratio, a disclination can decay into two intersecting disclinations, subsequently reducing the total energy of the system. Similar

phenomenon were observed experimentally for the case of translational decay of a disclination, for example, in decahedral particles containing one wedge positive disclination with a strength of 0.128 rad the decay of the disclination in two ones with parallel axes, was recorded during the growth of particles [42].

4. Conclusions

Thus, the study presents a calculation of the pair interaction energies of two intersecting defects. In the first part of the study, the specific energy of intersecting dilatation lines was determined in dependence on the angle between the lines of defects. It was shown that the energy of the pair interactions of intersecting dilatation lines takes a finite value, completely determined by the fields of defects in the vicinity of the intersection point. In the second part of the study, the interaction energy of intersecting wedge disclinations is found as the sum of two components: the first component contains the logarithmic singularity of the radial coordinate attributed to elastic fields and energies of disclination-type defects, the second term demonstrates the influence of the angle between the disclination axes on their interaction energy. The latter term is discussed in detail in the study. For instance, it was

demonstrated that disclinations intersecting under right angles have less interaction energy than disclinations with coincided axes. In addition, it was shown that the interaction energy of intersecting disclinations strongly depends on the properties of the elastic medium viz the Poisson ratio. For example, the higher Poisson ratio of the media the higher pair interaction energy of disclinations. The interaction energy of intersecting disclinations can take negative values in media with a relatively small Poisson ratio ($\nu < 0.2$). Probably, in the media with relatively small Poisson ratio the disclination could decay in two intersecting disclinations decreasing the total energy. In conclusion, it is worth noting that the obtained analytical relations for the pair interaction energy of intersecting dilatation lines and disclinations are of practical interest for further research, in particular, to employ construction of in theoretical modelling of residual stresses relaxation in icosahedral particles containing 6 intersecting wedge disclinations with a strength of 0.128 rad due to the impurity segregation at the cores of the disclinations.

Contribution of the authors

The authors contributed equally to this article.

Conflict of interests

The authors declare that they have no known competing financial interests or personal relationships that could have influenced the work reported in this paper.

References

1. Martinez A. D., Fioretti A. N., Toberer E. S., Tamboli A. C. Synthesis, structure, and optoelectronic properties of II–IV–V₂ materials. *Journal of Materials Chemistry A*. 2017;5(23): 11418–11435. <https://doi.org/10.1039/C7TA00406K>
2. Zhou H., Xu J., Liu X., ... Fan T. Bio-inspired photonic materials: Prototypes and structural effect designs for applications in solar energy manipulation. *Advanced Functional Materials*. 2018;28(24): 1705309. <https://doi.org/10.1002/adfm.201705309>
3. Shao L., Zhuo X., Wang J. Advanced plasmonic materials for dynamic color display. *Advanced Materials*. 2018;30(16): 1704338. <https://doi.org/10.1002/adma.201704338>
4. Matthews J. W., Blakeslee A. E. Defects in epitaxial multilayers: I. Misfit dislocations. *Journal of*

Crystal Growth. 1984;27: 118–125. [https://doi.org/10.1016/S0022-0248\(74\)80055-2](https://doi.org/10.1016/S0022-0248(74)80055-2)

5. Freund L. B., Suresh S. *Thin film materials: stress, defect formation and surface evolution*. Cambridge: Cambridge University Press; 2003. 803 p. <https://doi.org/10.1017/CBO9780511754715>

6. Gutkin M. Yu., Kolesnikova A. L., Romanov A. E. Nanomechanics of stress relaxation in composite low-dimensional structures. *Encyclopedia of Continuum Mechanics*. 2020: 1778–1799. https://doi.org/10.1007/978-3-662-55771-6_161

7. Smirnov A. M., Kremleva A. V., Ivanov A. Yu., ... Romanov A. E. Stress-strain state and piezoelectric polarization in orthorhombic Ga₂O₃ thin films depending on growth orientation. *Materials and Design*. 2023;226: 111616. <https://doi.org/10.1016/j.matdes.2023.111616>

8. Kukushkin S. A., Osipov A. V. A new mechanism of elastic energy relaxation in heteroepitaxy of monocrystalline films: Interaction of point defects and dilatation dipoles. *Mechanics of Solids*. 2013;48: 216–227. <https://doi.org/10.3103/S0025654413020143>

9. Ramdani R., Hounkpati V., Chen J., Ruterana P. Stress relaxation in III–V nitrides: investigation of metallic atoms interaction with the N-vacancy. *Europhysics Letters*. 2022;137(6): 66003. <https://doi.org/10.1209/0295-5075/ac6067>

10. Gutkin M. Yu., Kolesnikova A. L., Romanov A. E. Misfit dislocations and other defects in thin films. *Materials Science and Engineering: A*. 1993;164(1-2): 433–437. [https://doi.org/10.1016/0921-5093\(93\)90707-L](https://doi.org/10.1016/0921-5093(93)90707-L)

11. Bobylev S. V., Morozov N. F., Ovid'Ko I. A., Semenov B. N., Sheinerman A. G. Misfit dislocation configurations at interphase boundaries between misoriented crystals in nanoscale film-substrate systems. *Reviews on Advanced Materials Science*. 2012;32(1): 24–33.

12. Gutkin M. Yu., Kolesnikova A. L., Krasnitckii S. A., Romanov A. E., Shalkovskii A. G. Misfit dislocation loops in hollow core-shell nanoparticles. *Scripta Materialia*. 2014;83: 1–4. <https://doi.org/10.1016/j.scriptamat.2014.03.005>

13. Kukushkin S. A., Osipov A. V., Bessolov V. N., Konenkova E. V., Panteleev V. N. Misfit dislocation locking and rotation during gallium nitride growth on SiC/Si substrates. *Physics of the Solid State*. 2017;59(4): 674–681. <https://doi.org/10.1134/S1063783417040114>

14. Krasnitckii S. A., Smirnov A. M., Gutkin M. Yu. Axial misfit stress relaxation in core-shell nanowires with polyhedral cores through the nucleation of misfit prismatic dislocation loops. *Journal of Materials Science*. 2020;55: 9198–9210. <https://doi.org/10.1007/s10853-020-04401-3>

15. Smirnov A. M., Krasnitckii S. A., Gutkin M. Yu. Generation of misfit dislocations in a core-shell

- nanowire near the edge of prismatic core. *Acta Materialia*. 2020;186: 494–510. <https://doi.org/10.1016/j.actamat.2020.01.018>
16. Smirnov A. M., Krasnitckii S. A., Rochas S. S., Gutkin M. Yu. Critical Conditions of Dislocation Generation in Core-Shell Nanowires: A Review. *Reviews on Advanced Materials and Technologies*. 2020;2(3): 19–43. <https://doi.org/10.17586/2687-0568-2020-2-3-19-4>
17. Smirnov A. M., Young E. C., Bougrov V. E., Speck J. S., Romanov A. E. Stress relaxation in semipolar and nonpolar III-nitride heterostructures by formation of misfit dislocations of various origin. *Journal of Applied Physics*. 2019;126(24): 245104. <https://doi.org/10.1063/1.5126195>
18. Sheinerman A. G., Gutkin M. Yu. Misfit disclinations and dislocation walls in a two-phase cylindrical composite. *Physica Status Solidi (a)*. 2001;184(2): 485–505. [https://doi.org/10.1002/1521-396X\(200104\)184:2<485::AID-PSSA485>3.0.CO;2-4](https://doi.org/10.1002/1521-396X(200104)184:2<485::AID-PSSA485>3.0.CO;2-4)
19. Kolesnikova A. L., Ovidko I. A., Romanov A. E. Misfit disclination structures in nanocrystalline and polycrystalline films. *Solid State Phenomena*. 2002;87: 265–276. <https://doi.org/10.4028/www.scientific.net/SSP.87.265>
20. Skiba N. V., Ovid'ko I. A., Sheinerman A. G. Misfit disclination dipoles in nanocrystalline films and coatings. *Physics of the Solid State*. 2009;51(2): 280–285. <https://doi.org/10.1134/S1063783409020127>
21. Telyatnik R. S., Osipov A. V., Kukushkin S. A. Pore- and delamination-induced mismatch strain relaxation and conditions for the formation of dislocations, cracks, and buckles in the epitaxial AlN (0001)/SiC/Si (111) heterostructure. *Physics of the Solid State*. 2015;57(1): 162–172. <https://doi.org/10.1134/S106378341501031X>
22. Argunova T. S., Gutkin M. Yu., Mokhov E. N., Kazarova O. P., Lim J. H., Shcheglov M. P. Prevention of AlN crystal from cracking on SiC substrates by evaporation of the substrates. *Physics of the Solid State*. 2015;57(12): 2473–2478. <https://doi.org/10.1134/S1063783415120057>
23. Kukushkin S. A., Osipov A. V., Rozhavskaia M. M., Myasoedov A. V., Troshkov S. I., Lundin V. V., Sorokin L. M., Tsatsul'nikov A. F. Growth and structure of GaN layers on silicon carbide synthesized on a Si substrate by the substitution of atoms: a model of the formation of V-defects during the growth of GaN. *Physics of the Solid State*. 2015;57(9): 1899–1907. <https://doi.org/10.1134/S1063783415090218>
24. Schmidt V., McIntyre P. C., Gusele U. Morphological instability of misfit-strained core-shell nanowires. *Physical Review B*. 2008;77(23): 235302. <https://doi.org/10.1103/PhysRevB.77.235302>
25. Hofmeister H. Shape variations and anisotropic growth of multiply twinned nanoparticles. *Zeitschrift für Kristallographie*. 2009;224(11): 528–538. <https://doi.org/10.1524/zkri.2009.1034>
26. Ruditskiy A., Peng H. C., Xia Y. Shape-controlled metal nanocrystals for heterogeneous catalysis. *Annual Review of Chemical and Biomolecular Engineering*. 2016;7: 327–348. <https://doi.org/10.1146/annurev-chembioeng-080615-034503>
27. Romanov A. E., Kolesnikova A. L. Application of disclination concept to solid structures. *Progress in Materials Science*. 2009;54(6): 740–769. <https://doi.org/10.1016/j.pmatsci.2009.03.002>
28. Romanov A. E., Kolesnikova A. L. Elasticity boundary-value problems for straight wedge disclinations. A review on methods and results. *Reviews on Advanced Materials and Technologies*. 2021;3(1): 55–95. <https://doi.org/10.17586/2687-0568-2021-3-1-55-95>
29. Yasnikov I. S., Vikarchuk A. A. Voids in icosahedral small particles of an electrolytic metal. *JETP Letters*. 2006;83(1): 42–45. <https://doi.org/10.1134/S0021364006010103>
30. Huang J., Yan Y., Li X., Qiao X., Wu X., Li J., Shen R., Yang D., Zhang H. Unexpected Kirkendall effect in twinned icosahedral nanocrystals driven by strain gradient. *Nano Research*. 2020;13: 2641–2649. <https://doi.org/10.1007/s12274-020-2903-9>
31. Romanov A. E., Polonsky I. A., Gryaznov V. G., Nepijko S. A., Junghanns T., Vitrykhovski N. J. Voids and channels in pentagonal crystals. *Journal of Crystal Growth*. 1993;129(3-4): 691–698. [https://doi.org/10.1016/0022-0248\(93\)90505-Q](https://doi.org/10.1016/0022-0248(93)90505-Q)
32. Gutkin M. Yu., Panpurin, S. N. Spontaneous formation and equilibrium distribution of cylindrical quantum dots in atomically inhomogeneous pentagonal nanowires. *Journal of Macromolecular Science, Part B*. 2013;52(12): 1756–1769. <https://doi.org/10.1080/00222348.2013.808929>
33. Krasnitckii S. A., Gutkin M. Yu., Kolesnikova A. L., Romanov A. E. Formation of a pore as stress relaxation mechanism in decahedral small particles. *Letters on Materials*. 2022;12(2): 137–141. <https://doi.org/10.22226/2410-3535-2022-2-137-141>
34. Khramov A. S., Krasnitckii S. A., Smirnov A. M., Gutkin M. Yu. The void evolution kinetics driven by residual stress in icosahedral particles. *Materials Physics and Mechanics*. 2022;50(3): 401–409. https://doi.org/10.18149/MPM.5032022_4
35. Mura T. *Micromechanics of defects in solids*. Boston: Martinus Nijhoff Publishers; 1987. 587 p.
36. Kolesnikova A. L., Soroka R. M., Romanov A. E. Defects in the elastic continuum: classification, fields and physical analogies. *Materials Physics and Mechanics*. 2013;17(1): 71–91.
37. De Wit R. Partial disclinations. *Journal of Physics C: Solid State Physics*. 1972;5(5): 529–534. <https://doi.org/10.1088/0022-3719/5/5/004>

38. Vladimirov V. I., Romanov A. E. *Disclinations in Crystals*. Leningrad: Izdatel'stvo Nauka; 1986. 224p.

39. Kolesnikova A. L., Gutkin M. Yi., Proskura A. V., Morozov N. F., Romanov A. E. Elastic fields of straight wedge disclinations axially piercing bodies with spherical free surfaces. *International Journal of Solids and Structures*. 2016;99: 82–96. <https://doi.org/10.1016/j.ijsolstr.2016.06.029>

40. Prudnikov A. P., Brychkov I. A., Marichev O. I. *Integrals and series: special functions (Vol. 2)*. Amsterdam: Gordon and Breach Science Publishers; 1998. 740p.

41. Polonsky I. A., Romanov A. E., Gryaznov V. G., Kaprelov A. M. Disclination in an elastic sphere. *Philosophical Magazine A*. 1991;64(2): 281–287. <https://doi.org/10.1080/01418619108221185>

42. Mayoral A., Barron H., Estrada-Salas R., Vazquez-Duran A., Jos̄y-Yacam̄n M. Nanoparticle stability from the nano to the meso interval. *Nanoscale*. 2010;2(3): 335–342. <https://doi.org/10.1039/B9NR00287A>

Information about the authors

Stanislav A. Krasnitckii, Cand. Sci. (Phys.–Math.), Associate Professor at the Institute of Advanced Data Transfer Systems, ITMO University (St. Petersburg, Russian Federation).

<https://orcid.org/0000-0003-4363-8242>
krasnitsky@inbox.ru

Andrei M. Smirnov, Cand. Sci. (Phys.–Math.), Associate Professor at the Institute of Advanced Data Transfer Systems, ITMO University (St. Petersburg, Russian Federation).

<https://orcid.org/0000-0002-7962-6481>
smirnov.mech@gmail.com

Received 21.09.2023; approved after reviewing 28.09.2023; accepted for publication 16.10.2023; published online 25.12.2023.

Translated by Valentina Mittova